Scientific Research Publishing

Computational Chemistry, 2023, 11, 37-52
https://www.scirp.org/journal/cc
ISSN Online: 2332-5984
ISSN Print: 2332-5968

A TD-DFT Study for the Excited State Calculations of Microhydration of N-Acetyl-Phenylalaninylamide (NAPA)

Md. Alauddin*, Joya Dotta Ripa

Department of Theoretical and Computational Chemistry, University of Dhaka, Dhaka-1000, Bangladesh
Email: *alauddin1982@du.ac.bd

How to cite this paper: Alauddin, Md. and Ripa, J.D. (2023) A TD-DFT Study for the Excited State Calculations of Microhydration of N-Acetyl-Phenylalaninylamide (NAPA). *Computational Chemistry*, **11**, 37-52.
https://doi.org/10.4236/cc.2023.112003

Received: April 11, 2023
Accepted: April 25, 2023
Published: April 28, 2023

Abstract

Investigating the impact of microhydration on the excited-states and electronic excitation properties of biomolecules has remained one of the important yet challenging aspects of science because of the complexity of developing models. However, with the advent of computational chemistry methods such as TD-DFT, many useful insights about the electronic excitation energy and excited-state nature of biomolecules can be explored. Accordingly, in our study, we have incorporated the TD-DFT/*w*B97XD/cc-pVTZ method to study the excited state properties of N-acetyl phenylalanine amide (NAPA-A$(H_2O)_n$) (n = 1 to 4) clusters from ground to the tenth lowest gaseous singlet excited state. We found that the C=O bond length gradually increases both in N-terminal amide and C-terminal amide after the sequential addition of water molecules because of intermolecular H-bonding and this intermolecular H-bonding becomes weaker after the sequential addition of H_2O molecules. The UV absorption maxima of NAPA-A $(H_2O)_n$ (n = 1 - 4) clusters consisted of two peaks that are $S_5 \leftarrow S_0$ (1^{st} absorption) and $S_6 \leftarrow S_0$ (2^{nd} absorption) excitations. The first absorption maxima were blue-shifted with the increase in oscillator strength. This means that strong H-bonds reduce the charge transfer and make clusters more rigid. On the other hand, the second absorption maxima were red-shifted with the decrease in oscillator strength. In the ECD spectra, the negative bands indicate the presence of an amide bond and L-configuration of micro hydrated NAPA-A clusters. Finally, our calculated absorption and fluorescence energy confirm that all the NAPA-A $(H_2O)_n$ (n = 0 - 4) clusters revert to the ground state from the fluorescent state by emitting around 5.490 eV of light.

Keywords

Excited State, H-Bonding, Micro Hydration, Absorption and Fluorescence Energy

1. Introduction

Understanding the electronic states of potent biomolecules is becoming an active area of research in recent days [1] [2] [3]. Particularly, investigating the electronic transition characteristics of the biomolecules at the hydration interface while water molecules cluster around the macromolecules, is of the greatest area of interest both biologically and computationally because water is the main natural medium of the biological system and has an important impact on the structure of biomolecules [4]. Moreover, micro solvation is involved in many gas phase mechanisms where water molecules may have an influence on the structure and activity of the biomolecules due to the electrostatic interaction [5]. In protein, the aqueous environment has an impact on the binding ability of the amino acids because the clustering of water molecules has a tendency to accelerate the binding affinity of the amino acids to form a dipeptide bond. Moreover, surrounding water molecules sustained for a long time at the protein's active site are important for the selectivity and thermodynamic stability of ligands and protein binding. As a consequence, the hydration level has a profound impact on the dynamics of biomolecules [6].

Another important aspect of biomolecules' stability is the hydrogen bonding interaction (both intermolecular and intramolecular). Especially, studying intermolecular hydrogen bonding among the hydrogen bond donor and hydrogen bond acceptor atoms has gained popularity in recent years because these types of bonds are site-specific and play a vital role in physiochemical and biological procedures. Therefore, various theoretical and experimental methods are developed to study electronic ground state properties of intermolecular hydrogen bonding [7] [8] [9]. Hence, hydrogen bonding is involved in both the nonequilibrium mechanism of liquid and also in the photochemistry of chromophores at the solution phase. However, in the past, studying the electronic characteristics of hydrogen bonds in the excited states was difficult, and hence lack of scientific reports has been observed.

Recently, the advancement of computational chemistry methods has turned it possible to study the electronic transition states of biomolecules by implementing the time-dependent density functional theory (TD-DFT) method. This TD-DFT method has been proven as a useful tool to observe hydrogen bonding in accordance with the electronic transition to excited states [10]-[16]. This excitation can change the hydrogen bonding because of the difference in charge distribution in different electronic states.

This process is termed hydrogen bonding dynamics which is involved in many photochemical events in the hydrogen bonding process such as photo-induced electron transfer, vibrational energy relaxation, fluorescence quenching, and many more [17]. Moreover, studies have reported that reinforcing the excited state can decline the excitation energy in the relevant excitation state, and hence the absorption energy maximum shifts to the red. On the contrary, reducing hydrogen bonding energy may shift the absorption energy maximum to the blue

region [17]. Furthermore, to understand the folding of biological processes, depth insight into the structural and molecular rearrangement of H-bonding is necessary.

N-acetyl phenylalanine amide (NAPA) is a simple dipeptide model that is used to study the intermolecular and intramolecular interactions present among the native amino acid sites. Moreover, NAPA has intensive photophysical characteristics in the ultra-violet spectral range as there is an extensive aromatic side chain present with the core structure of NAPA. Plenty of experimental [18] and computational studies have reported on the structural motif and fluorescence quenching of NAPA [19]. Likewise, for the other chiral amino acids, the L-configuration of NAPA is more stable than the D-configuration. Furthermore, numeral theoretical and experimental studies on the L-configuration of NAPA has been proven that there are four stable conformers of NAPA namely NAPA-A, NAPA-B, NAPA-C, and NAPA-D [20]. Ramachandran angles of these conformers are $_{\beta}$L(a), γL(g+), γL(g-), and γL(a) respectively which identify their structural rearrangement. Nevertheless, among the conformers of NAPA, NAPA-A ($_{\beta}$L(a)) is the extended form of the peptide core structure and the most stable isomer because it contains an intermolecular C5 H-bond in accordance with NH···π interaction [5]. The Carbonyl group (-CO) and an amino group (-NH_2) present in the NAPA molecule make possible sites of hydrogen bonding with water molecules because these groups act as proton acceptors and donors at the same time. Therefore, like other micro-solvated biomolecules, the NAPA molecule acts like an organic chromophore as the molecule has competitive hydrogen bonding regions.

Here, in this study we investigate the hydrogen-bonded interaction of NAPA molecule with one to four water molecules [NAPA$(H_2O)_{1\text{-}4}$] positioned at various hydrogen bond-forming active sites using the TD-DFT method. Here, for our investigation, we have considered the most stable conformer of NAPA that is NAPA-A. We commence our investigation by putting the first water molecule strategically at (–CO) group end and then the (–NH) group end with a view to forming H-bonding interaction to stabilize the newly formed [NAPA$(H_2O)_1$] cluster. Afterward, the gradual number of water molecules is increased to four in a similar manner. We calculated the electronically excited states of [NAPA-A $(H_2O)_n$ (n = 4)] cluster in the gas phase to study the H-bonding properties and electronic characteristics of the clusters. This study is important to get a clear view of hydrogen bonding as well as to know the role of water on the structural and physiochemical modification of NAPA in the solvent environment. Therefore, this theoretical study where the explicit interaction of NAPA-A and few water molecules is considered as a microscopic model in gas-phase will play a pivotal role in future understanding of various solute (protein, DNA, RNA) and solvent (water) interactions in the biological system formed by a hydrogen bond. Moreover, along with the hydrogen bonding interaction we have studied the UV-Visible spectrum, and electronic circular dichroism (ECD) spectrum to clarify the properties of the excited states.

2. Computational Method

The geometry of NAPA-A and hydrated NAPA-A clusters were optimized by using Gaussian16 software packages [21] the and molecular geometry of the optimized structures was visualized by Gauss View 6.0. DFT method in accordance with dispersion correction functional (*w*B97XD) and more accurate cc-pVTZ basis set was used for optimizing the structures. Frequency calculation was also performed during the optimization using the same level of theory to confirm the minimized geometry of the structure. There was no imaginary frequency in optimized structures which ensures that the optimized geometry structures were minimum. Moreover, zero-point energy correction was also considered during the calculation. After that, electronic energy structures were calculated by using TD-DFT method utilizing *w*B97XD/cc-pVTZ functional because this functional is reported as accurate functional for predicting hydrogen bonding interaction as well as charge transfer in excitation states [22]. Then, with the same level of the theory underlying 10 excited singlet states of the clusters optimized S_0 geometries. Excited state dipole moments were calculated as it is very important to understand the excited state mechanism. In addition, UV-Visible and ECD spectra were also observed and data were tabulated for ten (10) exited states.

Electronic properties of the clusters such as frontier molecular orbitals (FMOs) (Highest Occupied molecular orbitals or HOMO and Lowest unoccupied molecular orbitals or LUMO) were also calculated by TD-DFT method. Gauss-sum 3.0 software was used for generating density of states (DOS) plots and interpreting oscillator strength and energy difference of the FMOs [23]. In order to generate graphs of UV-Visible and ECD spectra, Origin software (Origin. 2003. Origin 7.5. OriginLab Corp., Northampton, MA) was used.

3. Results and Discussion

3.1. Optimized Geometry: Bond Length, Intermolecular and Intramolecular Hydrogen Bonding

TD-DFT calculations were done on NAPA-A conformer with explicitly added four water molecules that are hydrogen bonded with the peptide itself or involved in a network of hydrogen bonds with adjacent water molecules. In both ground state (GS) and excited states (ES), calculated intra- and intermolecular hydrogen bond lengths of bare NAPA-A and NAPA-A water clusters are depicted in **Table 1**. From our calculation, we can see fluctuations have occurred in bond lengths of C=O with an explicit increase of water molecules in the system. In the optimized NAPA-A conformer without adding any water molecule, C=O bond lengths of N-terminal and C-terminal amide were 1.216 Å and 1.219 Å respectively. When water molecules have been added one to four in a sequential order for forming NAPA-A $(H_2O)_n$ clusters, the C=O bond length (N-terminal) changes to 1.224 Å, 1.228 Å, 1.241 Å, and 1.240 Å respectively and the C=O bond length (C-terminal) changes to 1.221 Å, 1.227 Å, 1.227 Å, and 1.236 Å

Table 1. Intra and inter-molecular hydrogen bond lengths (HBL) in the ground state (GS) and excited state (ES) of [NAPA-A $(H_2O)_n$ (n = 0 - 4)] clusters. Excited state bond lengths were calculated in the S_5 state.

	Intermolecular Hydrogen Bond (Å)			Intramolecular Hydrogen Bond (Å)		
Hydration Level	Bonds	HBL (GS)	HBL (ES)	Bonds	HBL (GS)	HBL (ES)
NAPA-A				O25-H17	2.155	2.155
				O19-H29	2.540	2.540
NAPA-A $(H_2O)_1$	O30-H17	2.029	2.029	O19-H28	2.324	2.324
	O25-H31	1.877	1.877			
NAPA-A $(H_2O)_2$	O30-H17	1.928	1.928			
	O19-H35	1.777	1.777			
	O25-H31	1.807	1.807			
	O33-H28	1.873	1.873			
NAPA-A $(H_2O)_3$	O30-H17	1.935	1.935			
	O19-H35	1.787	1.787			
	O25-H38	1.898	1.898			
	O25-H31	1.814	1.814			
	O33-H28	1.883	1.883			
	O36-H27	2.071	2.071			
NAPA-A $(H_2O)_4$	O30-H17	1.916	1.916			
	O19-H35	1.802	1.802			
	O25-H38	1.907	1.907			
	O25-H31	1.819	1.819			
	O33-H28	1.895	1.895			
	O36-H27	2.060	2.060			
	O19-H40	1.898	1.898			

respectively. This indicates the C=O bond length gradually increases both in N-terminal amide and C-terminal amide after the sequential addition of water molecules because of intermolecular hydrogen bonding.

Moreover, there was a significant fluctuation observed in intermolecular hydrogen bonding of the clusters when the hydration level was increased. As we already know that bare NAPA-A molecule form two intramolecular ring structures: 1) C5 hydrogen bonding network and 2) C7 hydrogen bonding network [24]. In NAPA-A $(H_2O)_1$ cluster, our calculations have shown that both intra- and intermolecular hydrogen bonding is present. The intermolecular hydrogen bonding between O30···H17 atoms and O25···H31 atoms are 2.029 Å and 1.877 Å respectively in both the ground state and excited state. On the other hand, the intramolecular hydrogen bond length between the O19···H28 atom is 2.324 Å. After the sequential addition of 2nd water molecule, there is no intramolecular

hydrogen bond in the hydrated cluster as both C5 and C7 ring positions are blocked by the water molecule. The intermolecular H-bond length between the oxygen of C-terminal amide and hydrogen of the H_2O molecule (O19···H35) increases gradually with the increase in cluster size. The H-bond lengths of O19···H35 for n = 2, 3 and 4 clusters are 1.777 Å, 1.787 Å and 1.802 Å, respectively. Similarly, the intermolecular H-bond length between the oxygen of N-terminal amide and hydrogen of H_2O (O25···H31) molecule also increases gradually. The H-bond lengths of O25···H31 for n = 2, 3 and 4 clusters are 1.807 Å, 1.814 Å and 1.819 Å, respectively. This consecutive increase in bond distances indicates the weakening of intermolecular hydrogen bonding due to a decrease in electron density in the carbonyl group of oxygen. This is an important phenomenon of a biological system as the interaction of protein in biological protic solvent water depends mostly on hydrogen bonding nature. On the other hand, a weaker intermolecular and a stronger intramolecular hydrogen bonding makes peptide residue more flexible to form bonds [25].

Moreover, the intermolecular H-bond distance between O33···H28 ($-NH_2\cdots OH_2$) for n = 2, 3 and 4 clusters are 1.873 Å, 1.883 Å and 1.895 Å, respectively. This also confirms that intermolecular H-bonding becomes weaker after the sequential addition of H_2O molecules in NAPA-A (**Figure 1**). But our calculated data have not shown any changes in the hydrogen bond distance of the ground state and excited state. As we know that TDDFT excitation occurs vertically, that's why there is no change in the bond distance.

3.2. Frontier Molecular Orbital Analysis

Frontier molecular orbitals (FMOs) are the minimum energy gap between the highest occupied molecular orbital (HOMO) and lowest unoccupied molecular orbital (LUMO). These FMOs are useful indicators of the optical and chemical properties of compounds as the electron affinity of the compound can be identified by observing LUMO whereas, the HOMO can be used to identify the ionization energy. The most important two factors of chemical compounds are stability and reactivity is also depended on the band gap of this HOMO and LUMO orbitals energy. The more will be the band gap of the compound the more will be its stability. On the contrary, compound with relatively lower band gaps are less stable and has impressive reactivity. The three-dimensional plot of FMOs of NAPA water clusters generated by TD-DFT/*w*B97XD/cc-pVTZ computational method is portrayed in **Figure 2**.

According to our calculation, it can be observed that the HOMO-LUMO energy gap is increased consecutively from one water molecule to four water molecules. In NAPA-A molecule the band gap is 10.14 eV. This band gap increased to 10.29 eV in NAPA-A $(H_2O)_1$ and this band gap remain constant in NAPA-A $(H_2O)_2$ as well. In NAPA-A $(H_2O)_3$ and NAPA-A $(H_2O)_4$ band gaps elevatedto 10.31 eV and 10.33 eV respectively. This high band gap of the NAPA-A $(H_2O)_4$ compound indicates that this cluster is highly stable. In addition, it can also be observed that the total density of HOMO is over the total

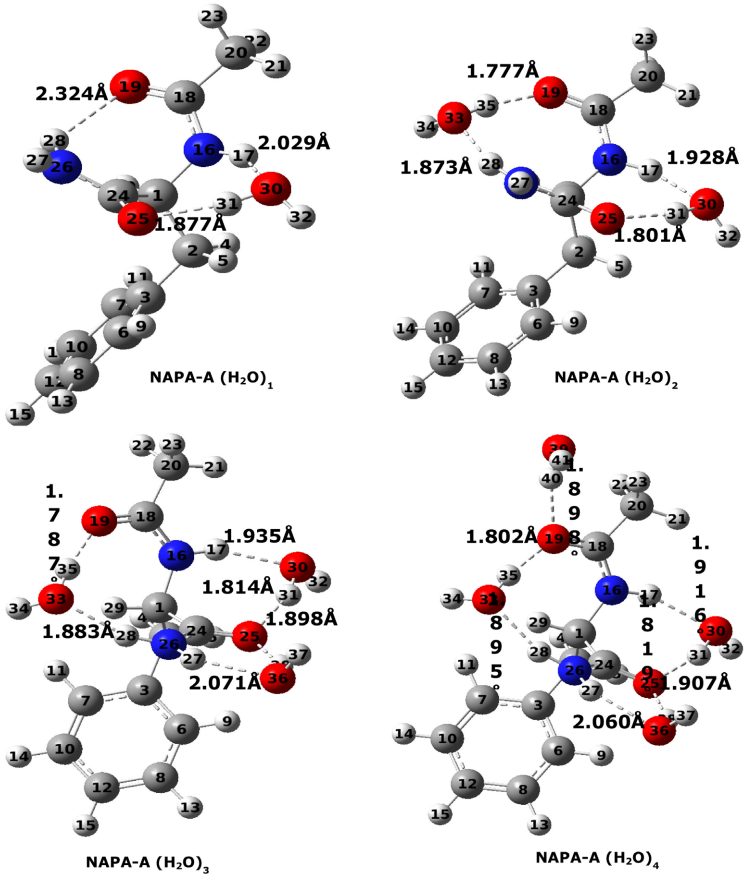

Figure 1. Representation of intermolecular and intramolecular hydrogen bonding in NAPA-A $(H_2O)_n$ (n = 1 - 4) clusters.

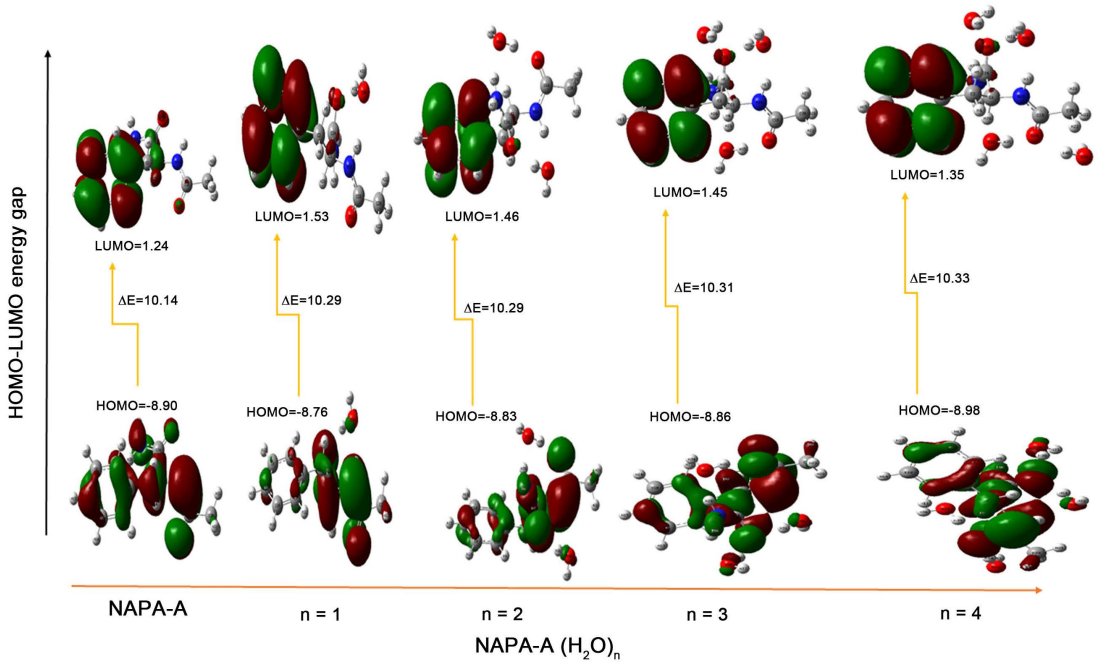

Figure 2. HOMO-LUMO energy gap of [NAPA-A $(H_2O)_n$ (n = 0 - 4)] clusters with TD-DFT/*ω*B97XD/cc-pVTZ method.

molecules. However, the density of LUMO is confined to the phenyl ring only and particularly on the C-C-O pan. This FMOs analysis unravels the charge transfer from the peptide backbone of NAPA-A to the phenyl ring. The total density of states (DOS) diagram of NAPA-A $(H_2O)_n$ clusters is portrayed in Figure 3.

3.3. Electronic Transition Properties (UV-Visible and ECD Spectrum)

The electronic transition properties of micro hydrated NAPA water clusters can be calculated by the TD-DFT method. The TD-DFT approach is widely used for its high level of accuracy, cost-effectiveness, and low time requirements. TD-DFT/*ω*B97XD/cc-pVTZ computational method is used to calculate the ten lowest singlet excited states in the gas phase. Excitation energy (eV), absorption wavelength (nm), oscillator strength (f), nature of the transition, and major contributions of molecular orbitals are generated using Gauss-Sum 3.0 software and represented in Table 2.

The electronic absorption of compounds differs mainly on the characteristics of the ground state and first excited state. Predominantly, photoexcitation of electrons from their HOMO energy state to LUMO determines the electronic absorption. Here, in our study, we considered excitation energy from the ground to the first, fifth, and sixth excited states with their excited state dipole moment to compare the excitation nature of the NAPA-A and NAPA-A water clusters in the gaseous states. In the NAPA-A compound without any micro hydration, the first electronic transition from the ground state (S_0) to the first excited state (S_1) was calculated at 226.55 nm (5.472 nm) with 0.0015 oscillator strength. This transition reflects the transition character of n to π* and slight charge transfer (CT) from amino acid to the phenyl ring with the molecular contribution of H-2- > L (21%), H-2- > L + 1 (20%), H- > L (19%), H- > L + 1 (24%). The dipole moments of the ground state (S_0) and the first excited state (S_1) are 2.578 D and 2.432 D, respectively (Table 2). The ($S_5 \leftarrow S_0$) transition is predicted at 180.25 nm (6.878) with the strongest oscillator strength (0.482) among the ten excited states. This is π to π* transition with the molecular contribution of H-2- > L + 1 (24%) and H- > L (24%). The second strongest transition with an oscillator strength of 0.378 is predicted at 176.92 nm. It also reflects π to π* transition with slight charge transfer and dipole moment decreases.

Accordingly, using the TD-DFT method excited states nature of the NAPA-A water clusters was calculated during our study. Likewise, the NAPA-A conformer, excitation energy from S_0 to S_1, S_5 and S_6 are considered. In NAPA-A $(H_2O)_1$ the first excitation from $S_0 \rightarrow S_1$ occurs at 225.52 nm (5.497 eV) with 0.0008 oscillator strength. While the number of water molecules has been increased consecutively to four, fluctuation of absorption wavelength was observed. The wavelength for excitation in first excited states for the clusters of NAPA-A $(H_2O)_n$ (n = 1 - 4) was calculated at 225.52 nm (5.497 eV), 225.80 nm (5.490 eV), 225.81 nm (5.490 eV), 225.77 nm (5.491 eV) with a successively

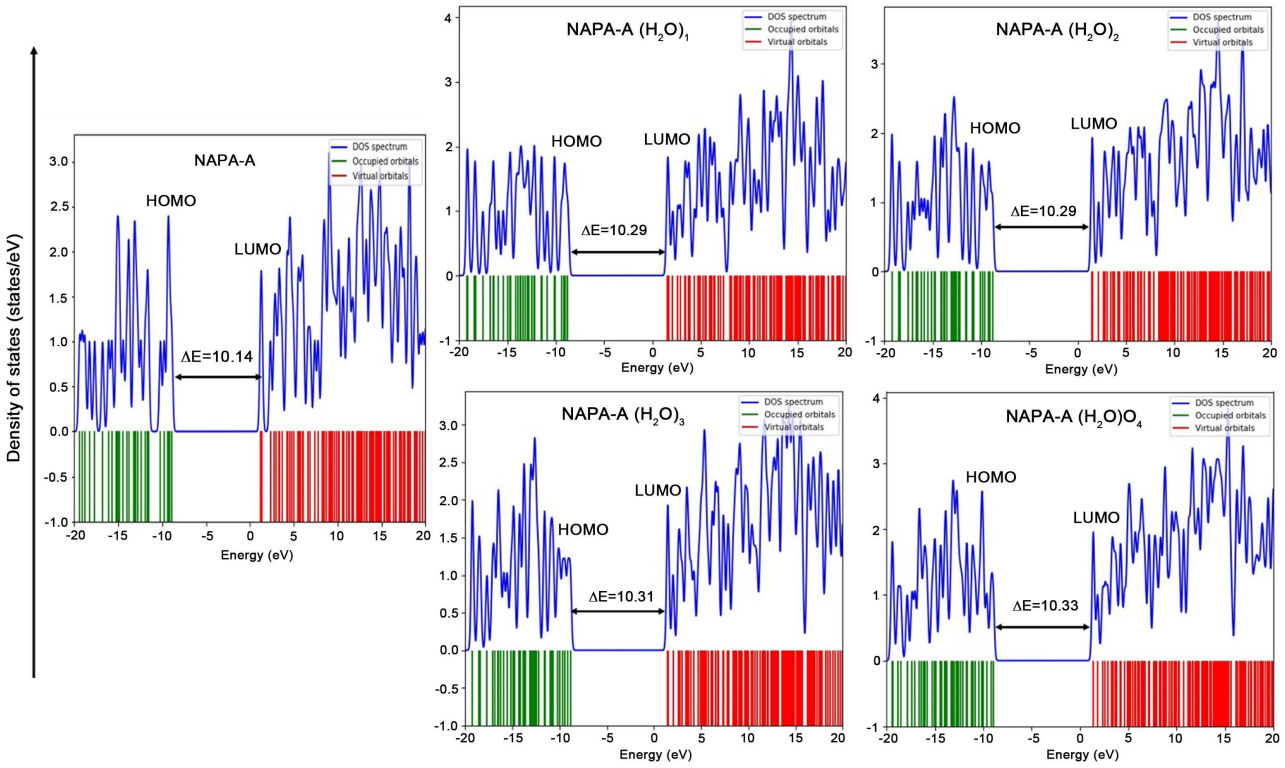

Figure 3. DOS diagram of NAPA-A $(H_2O)_n$ with TD-DFT/*w*B97XD/cc-pVTZ computational method.

Table 2. The UV and ECD spectra of the ten lowest excited states of NAPA-A $(H_2O)_n$ clusters by applying the photoexcitation implementing TD-DFT/wB97XD/cc-pVTZ method.

	UV spectrum				ECD			
Cluster	λ_{max} (nm)	Excited state (*)	NT	OS (f)	Energy (eV)	λ (nm)	R (Vel)	Major Contribution (≥10%)
NAPA-A	226.55	S_0 (2.578)→S_1 (2.432)	n→π* and CT	0.0015	5.472	226.55	−0.030	H-2- > L (21%), H-2- > L + 1 (20%), H- > L (19%), H- > L + 1 (24%)
	180.25	S_0 (2.578)→S_5 (1.666)	π→π*	0.482	6.878	180.25	−72.81	H-2- > L + 1 (24%), H- > L (24%)
	176.92	S_0 (2.578)→S_6 (1.940)	π→π* and CT	0.378	7.008	176.92	−49.92	H-2- > L (39%), H- > L + 1 (34%)
NAPA-A $(H_2O)_1$	225.52	S_0 (0.955)→S_1 (0.944)	n→π* and CT	0.0008	5.497	225.52	+0.405	H-1- > L (28%), H-1- > L + 1 (15%), H- > L (28%), H- > L + 1 (24%)
	176.26	S_0 (0.955)→S_5 (0.986)	π→π*	0.777	7.034	176.26	+51.82	H-1- > L + 1 (46%), H- > L (30%)
	175.53	S_0 (0.955)→S_6 (1.101)	π→π* and CT	0.491	7.063	175.53	−86.39	H-1- > L (35%), H- > L + 1 (33%)
NAPA-A $(H_2O)_2$	225.80	S_0 (2.033)→S_1 (1.966)	n→π* and CT	0.0007	5.490	225.80	−0.381	H-1- > L (24%), H-1- > L + 1 (19%), H- > L (26%), H- > L + 1 (20%)
	176.74	S_0 (2.033)→S_5 (1.338)	π→π*	0.841	7.015	176.74	−35.84	H-1- > (22%), H-1- > L + 1 (30%), H- > L(18%), H- > L + 1 (18%)
	175.91	S_0 (2.033)→S_6 (2.224)	π→π* and CT	0.398	7.048	175.91	−3.91	H-1- > L (24%), H-1- > L + 1 (26%), H- > L (20%), H- > L + 1 (23%)

Continued

NAPA-A $(H_2O)_3$	225.81	S_0 (2.464)→S_1 (2.423)	n→π* and CT	0.0006	5.490	225.81	−0.23	H-1- > L (20%), H-1- > L + 1 (24%), H- > L (30%), H- > L + 1 (18%)
	176.59	S_0 (2.464)→S_5 (2.378)	π→π*	0.850	7.021	176.59	−43.03	H-1- > L (26%), H-1- > L + 1 (29%), H > L (17%), H- > L + 1 (19%)
	176.21	S_0 (2.464)→S_6 (3.144)	π→π* and CT	0.376	7.036	176.21	−14.10	H-1- > L (20%), H-1- > L + 1 (26%), H- > L (22%), H- > L + 1 (21%)
NAPA-A $(H_2O)_4$	225.77	S_0 (2.934)→S_1 (2.962)	n→π* and CT	0.0005	5.491	225.77	−0.237	H-1- > L (18%), H-1- > L + 1 (26%), H- > L (32%), H- > L + 1 (17%)
	176.58	S_0 (2.934)→S_5 (2.914)	π→π*	0.905	7.021	176.58	−43.02	H-1- > L (30%), H-1- > L + 1 (23%), H- > L (13%), H- > L + 1 (22%)
	176.30	S_0 (2.934)→S6 (3.343)	π→π* and CT	0.348	7.033	176.30	−14.09	H-1- > L (15%), H-1- > L + 1 (30%), H- > L (27%), H- > L + 1 (18%)

* = excited state dipole moment, NT = Nature of transition, OS = Oscillator strength, λ = wavelength, R_{vel} = Rotational strength (dipole velocity), CT = Charge transfer, H = HUMO and L = LOMO.

decreased oscillator strengths 0.0008, 0.0007, 0.006 and 0.0005 respectively. Unlikely, with the NAPA-A S_1 excited states, all of the cluster's photoexcitation from S_0 to the S_1 state corresponds from HOMO→LUMO with 28%, 26%, 30%, and 32% major contributions. Nevertheless, a subtle change in the wavelength of the clusters in the gas phase S_5 excited state where the oscillator strength was the strongest. Absorption maxima of NAPA-A $(H_2O)_n$ (n = 1 - 4) clusters were predicted (S_5←S_0 excitation) computationally at 176.26 nm (7.034 eV), 176.74 nm (7.015 eV), 176.59 nm (7.021 eV), and 176.58 nm (7.021eV) respectively with a continuous stronger elevated oscillator strength of 0.777, 0.841, 0.850 and 0.905. The transition nature for S_5←S_0 excitation is π to π* with combined molecular orbital contributions of H-1 to L, H-1 to L + 1, H to L, and H to L + 1. For all n = 1 to 4 clusters, the excited state dipole moments are lower compared to the ground state dipole moment.

An interesting phenomenon is observed for S_6←S_0 electronic excitation of NAPA-A $(H_2O)_n$ (n = 1 - 4) clusters. The second absorption maxima were predicted at 175.53 nm (7.063 eV), 175.91 nm (7.048 eV), 176.21 nm (7.036 eV), and 176.30 nm (7.033 eV) for n= 1, 2, 3 and 4 clusters respectively with a continuous weaker oscillator strength of 0.491, 0.398, 0.376 and 0.348. The second λ_{max} red-shifted due to the charge transfer from the ground state to the sixth electronic excited state. The dipole moments of the ground state (S_0) are 0.955, 2.033, 2.464, 2.934 D and the sixth excited state (S_6) are 1.101, 2.224, 3.144, and 3.343 D for n = 1, 2, 3, 4 respectively. This dipole moment enhancement in the sixth excited state indicates that charge transfer occurred in the sixth excited state. Our calculation predicts that the second absorption maxima red-shifted

with increasing the hydration level in the gaseous phase. Figure 4 is depicting the shifting of wavelength after the explicit addition of water molecules to the NAPA-A.M. Mons and his coworkers extensively studied experimentally both bare NAPA and monohydrated NAPA complexes. They reported using resonance two-photon ionization (R2PI) spectroscopy that the first electronic transition (π to π^*) for bare NAPA is observed at 266.62 nm and it is blue-shifted (266.13 nm) for monohydrated NAPA complex [20]. Similar results were also found in our calculations.

On the contrary, the ECD spectrum was calculated theoretically at the same level of theory and listed in Table 2. An ECD spectrum is the graphical representation of ellipticity changes ($\Delta\varepsilon$) against wavelength (λ). In the ECD spectrum, the positive cotton effect (CE) is observed when the peak tends to shorter wavelength than the trough. Alternatively, when the peak inclines to a longer wavelength, negative CE is observed. Normally, enantiomers that are optically pure show a negative CE effect. According to the previous study, it is known that amide groups show UV and ECD transition spectrum at far-UV region (180 - 250 nm) [26]. In NAPA-A conformer at 180.25 nm strong CE was observed with a negative band ($\Delta\varepsilon = -72.81$). Similarly, at 180.25 nm strong peak is observed which mainly originates from then→π^* transition of chromophores of thephenyl ring of NAPA-Aand the lone pair electron of oxygen to π antibonding orbital (N-C=O). Hence, the negative band ($\Delta\varepsilon = -72.81$) at 180.25 nm in the calculated ECD spectrum clarifies the presence of the amide bond in the NAPA-A compound. Among the clusters of NAPA-A water, only NAPA-A $(H_2O)_1$ shows two positive CE ($S_1 \leftarrow S_0$ and $S_5 \leftarrow S_0$) bands at 225.52 nm ($\Delta\varepsilon = +0.405$) and 176.26 nm ($\Delta\varepsilon = +51.82$) anda strong negative CE band ($\Delta\varepsilon = -86.39$) at 175.53 nm. However, all the other clusters such as NAPA-A $(H_2O)_2$, NAPA-A $(H_2O)_3$, and NAPA-A $(H_2O)_4$ show three negative CE bands. The UV and ECD spectra of n = 0 to 4 clusters are shown in Figure 5.

3.4. Analysis of Absorption and Emission Energy

Absorption and emission energy have been calculated using TD-DFT/*ω*B97XD/cc-pVTZ level of computational approach for NAPA-A $(H_2O)_n$ (n = 0 - 4) clusters in the gas phase and data were tabulated in Table 3.

We mentioned in Table 2 that the first electronic transition of all the clusters reflects the transition character of n to π^* which means electron density increases in the S_1 excited state. Lan *et al.* reported that intramolecular hydrogen bonding becomes significantly strengthened in the S_1 stateupon photo-excitation [27]. It is now well established that excited state hydrogen bond strengthening facilitates internal conversion (IC) from the fluorescent state to the ground state [28]. The absorption energy of NAPA-A is 6.878 eV and it increases for the hydrated clusters which are around 7.021 eV. This absorption energy is calculated on the basis of the S_0 to S_5 electronic transition. On the other way, the emission energy of NAPA-A is 5.472 eV and it decreases for the hydrated clusters which are around 5.490 eV. This calculation predicts that all the hydrated clusters dissipated

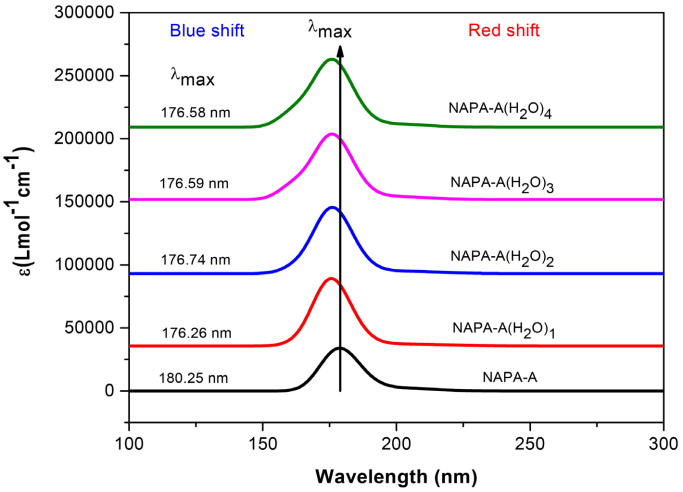

Figure 4. Diagram of wavelength shifting of NAPA-A $(H_2O)_n$ (n = 0 to 4) clusters in gaseous phase computed by TD-DFT/*w*B97XD/cc-pVTZ method.

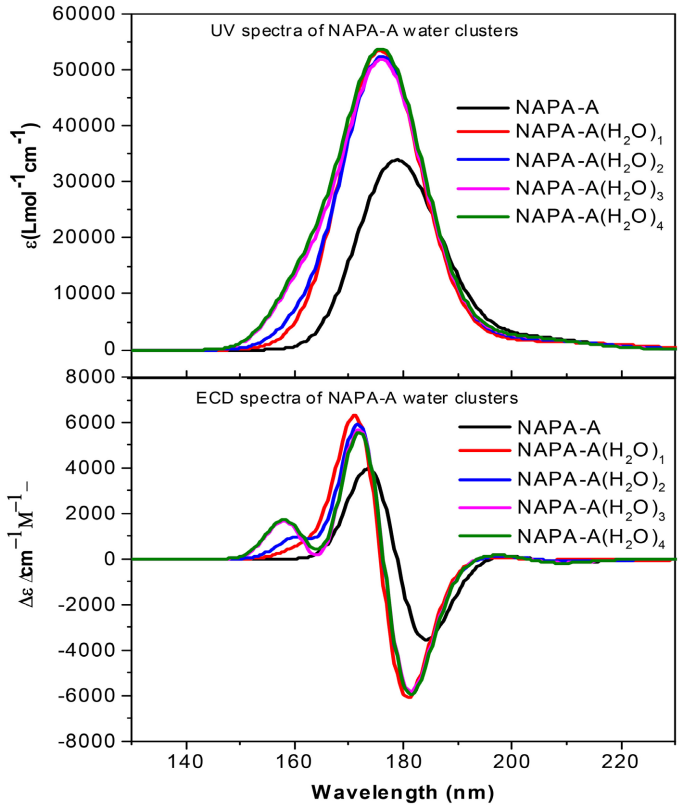

Figure 5. UV (upper figure) and ECD (lower figure) spectrum of NAPA-A $(H_2O)_n$ (n = 0 - 4).

around 1.531 eV of energy to fall S_1 electronic state from the S_5 electronic state. The calculated emission energy is basically fluorescence energy as we calculated the energy from the S_1 state to the S_0 state. Finally, NAPA-A $(H_2O)_n$ (n = 0 - 4) clusters revert to the ground state from the fluorescent state by emitting 5.490 eV of light.

Table 3. Computed absorption and emission energy of NAPA-A $(H_2O)_n$ (n = 0 - 4) clusters in the gas phase.

Cluster	Absorption energy (eV)	Emission energy (eV)
NAPA-A	6.878	5.472
NAPA-A $(H_2O)_1$	7.034	5.497
NAPA-A $(H_2O)_2$	7.015	5.490
NAPA-A $(H_2O)_3$	7.021	5.490
NAPA-A $(H_2O)_4$	7.021	5.491

4. Conclusion

The TDDFT/*w*B97XD/cc-pVTZ computational methods were applied to understand the changes in H-bonding and electronic properties of [NAPA-A $(H_2O)_n$ n = 1 - 4] clusters. Our calculations suggest that the C=O bond length gradually increases both in N-terminal amide and C-terminal amide after the sequential addition of water molecules because of intermolecular hydrogen bonding. Moreover, the intermolecular H-bonding becomes weaker after the sequential addition of H_2O molecules in NAPA-A. But the hydrogen bond distance of the ground state and the excited state has no change as the TDDFT excitation occurs vertically. From the analysis of FMO's and TDOS data, it reveals that the charge transfer occurred from the peptide backbone of NAPA-A to the phenyl ring. The absorption maxima of NAPA-A $(H_2O)_n$ (n = 1 - 4) clusters were predicted at 176.26, 176.74, 176.59, and 176.58 nm respectively with a continuous stronger elevated oscillator strength of 0.777, 0.841, 0.850 and 0.905. Interestingly, the excited state dipole moments are lower compared to the ground state dipole moment for all the clusters. On the other hand, the second absorption maxima were predicted at 175.53, 175.91, 176.21, and 176.30 nm for n = 1, 2, 3 and 4 clusters respectively with a continuous weaker oscillator strength of 0.491, 0.398, 0.376 and 0.348. In our study, among the NAPA-A $(H_2O)_n$ (n = 1 - 4) clusters, only NAPA-A $(H_2O)_1$ shows two positive CE bands at 225.52 and 176.26 nm and a strong negative CE band at 175.53 nm. However, all the other clusters show three negative CE bands. These negative bands indicate the presence of an amide bond and L-configuration of micro hydrated NAPA-A clusters. Finally, our calculated absorption and fluorescence energy confirm that all the NAPA-A $(H_2O)_n$ (n = 0 - 4) clusters revert to the ground state from the fluorescent state by emitting around 5.490 eV of light.

Acknowledgement

This work was supported by Centennial Research Grant, University of Dhaka (CRG-DU) (2nd Phase).

Conflicts of Interest

The authors declare no conflicts of interest regarding the publication of this paper.

References

[1] Level, M., Very, T., Gloaguen, E., Tardivel, B., Mons, M. and Brenner, V. (2022) Excited States Computation of Models of Phenylalanine Protein Chains: TD-DFT and Composite CC2/TD-DFT Protocols. *International Journal of Molecular Sciences*, **23**, Article No. 621. https://doi.org/10.3390/ijms23020621

[2] Stephens, A.D., Qaisrani, M.N., Ruggiero, M.T., Mirónf, G.D., Morzan, U.N., Lebrero, M.C.G., Jones, S.T.E., Poli, E., Bond, A.D., Woodhams, P.J., Kleist, E.M., Grisanti, L., Gebauer, R., Zeitler, J.A., Credgington, D., Hasanali, A. and Schierle, G.S.K. (2021) Short Hydrogen Bonds Enhance Nonaromatic Protein-Related Fluorescence. *Proceedings of the National Academy of Sciences*, **118**, e2020389118. https://doi.org/10.1073/pnas.2020389118

[3] Kerdpol, K., Daengngern, R., Sattayanon, C., Namuangruk, S., Rungrotmongkol, T., Wolschann, P., Kungwan, N. and Hannongbua, P. (2021) Effect of Water Microsolvation on the Excited-State Proton Transfer of 3-Hydroxyflavone Enclosed in γ-Cyclodextrin. *Molecules*, **26**, Article No. 843. https://doi.org/10.3390/molecules26040843

[4] Nagornova, N.S., Rizzo, T.R. and Boyarkin, O.V. (2012) Interplay of Intra- and Intermolecular H-Bonding in a Progressively Solvated Macrocyclic Peptide. *Science*, **336**, 320-323. https://doi.org/10.1126/science.1218709

[5] Barron, L.D. (2015) The Development of Biomolecular Raman Optical Activity Spectroscopy. *Biomedical Spectroscopy and Imaging*, **4**, 223-253. https://doi.org/10.3233/BSI-150113

[6] Biedermannová, L. and Schneider, B. (2016) Hydration of Proteins and Nucleic Acids: Advances in Experiment and Theory. A Review. *Biochimica et Biophysica Acta* (*BBA*)-*General Subjects*, **1860**, 1821-1835. https://doi.org/10.1016/j.bbagen.2016.05.036

[7] Cheng, C.-L. and Zhao, G.-J. (2012) Steered Molecular Dynamics Simulation Study on Dynamic Self-Assembly of Single-Stranded DNA with Double-Walled Carbon Nanotube and Graphene. *Nanoscale*, **4**, 2301-2305. https://doi.org/10.1039/c2nr12112c

[8] Cheng, C.-L., Zhang, M.-Z. and Zhao, G.-J. (2014) Mechanical Stability and Thermal Conductivity of β-Barrel in Green Fluorescent Protein by Steered Molecular Dynamics. *RSC Advances*, **4**, 6513-6516. https://doi.org/10.1039/c3ra42679c

[9] Zhang, M.-X., Chai, S. and Zhao, G.-J. (2012) BODIPY Derivatives as n-Type Organic Semiconductors: Isomer Effect on Carrier Mobility. *Organic Electronics*, **13**, 215-221. https://doi.org/10.1016/j.orgel.2011.10.015

[10] Li, H., Liu, Y., Yang, Y., Yang, D. and Sun, J. (2014) Excited-State Intramolecular Hydrogen Bonding of Compounds Based on 2-(2-Hydroxyphenyl)-1,3-benzoxazole in Solution: A TDDFT Study. *Spectrochimica Acta Part A*: *Molecular and Biomolecular Spectroscopy*, **133**, 818-824. https://doi.org/10.1016/j.saa.2014.06.072

[11] Liu, X., Yin, H., Li, H. and Shi, Y. (2017) Altering Intra- to Inter-Molecular Hydrogen Bonding by Dimethylsulfoxide: A TDDFT Study of Charge Transfer for Coumarin 343. *Spectrochimica Acta Part A*: *Molecular and Biomolecular Spectroscopy*, **177**, 1-5. https://doi.org/10.1016/j.saa.2017.01.022

[12] Wang, P., Song, X., Zhao, Z., Liu, L., Mu, W. and Hao, C. (2016) Role of the Electronic Excited-State Hydrogen Bonding in the Nitro-Explosives Detection by $[Zn_2(oba)_2(bpy)]$. *Chemical Physics Letters*, **661**, 257-262. https://doi.org/10.1016/j.cplett.2016.06.085

[13] Ji, M., Hao, C., Wang, D., Li, H. and Qiu, J. (2013) A Time-Dependent Density Functional Theory Study on the Effect of Electronic Excited-State Hydrogen Bonding on Luminescent MOFs. *Dalton Transactions*, **42**, 3464-3470. https://doi.org/10.1039/C2DT32575F

[14] Li, H., Liu, Y., Yang, Y., Yang, D. and Sun, J. (2014) Influences of Hydrogen Bonding Dynamics on Adsorption of Ethyl Mercaptan onto Functionalized Activated Carbons: A DFT/TDDFT Study. *Journal of Photochemistry and Photobiology A*: *Chemistry*, **291**, 9-15. https://doi.org/10.1016/j.jphotochem.2014.06.017

[15] Li, H., Yang, Y., Yang, D., Liu, Y. and Sun, J. (2014) TDDFT Study on the Excited State Hydrogen Bonding of N-(2-hydroxyethyl)-1,8-naphthalimide and N-(3-hydroxyethyl)-1,8-naphthalimide in Methanol Solution. *Journal of Physical Organic Chemistry*, **27**, 170-176. https://doi.org/10.1002/poc.3255

[16] Wei, N., Hamza, A., Hao, C., Xiu, Z. and Qiu, J. (2013) Time-Dependent Density Functional Theory Study on Hydrogen and Dihydrogen Bonding in Electronically Excited State of 2-Pyridone-Borane-Trimethylamine Cluster. *Journal of Cluster Science*, **24**, 459-470. https://doi.org/10.1007/s10876-013-0572-5

[17] Yang, D., Zheng, R. and Lv, J. (2017) Hydrogen Bonding and Excited State Properties of the Photoexcited Hydrogen-Bonded (*E*)-S-(2-aminopropyl) 3-(4-hydroxyphenyl)prop-2-enethioate Complexes. *Journal of Physical Organic Chemistry*, **30**, e3634. https://doi.org/10.1002/poc.3634

[18] Mališ, M., Loquais, Y., Gloaguen, E., Jouvet, C., Brenner, V., Mons, M., Ljubić, I. and Došlić, N. (2014) Non-Radiative Relaxation of UV Photoexcited Phenylalanine Residues: Probing the Role of Conical Intersections by Chemical Substitution. *Physical Chemistry Chemical Physics*, **16**, 2285-2288. https://doi.org/10.1039/c3cp53953a

[19] Mališ, M. and Došlić, N. (2017) Nonradiative Relaxation Mechanisms of UV Excited Phenylalanine Residues: A Comparative Computational Study. *Molecules*, **22**, Article No. 493. https://doi.org/10.3390/molecules22030493

[20] Biswal, H.S., Loquais, Y., Tardivel, B., Gloaguen, E. and Mons, M. (2011) Isolated Monohydrates of a Model Peptide Chain: Effect of a First Water Molecule on the Secondary Structure of a Capped Phenylalanine. *Journal of the American Chemical Society*, **133**, 3931-3942. https://doi.org/10.1021/ja108643p

[21] Frisch, M.J., Trucks, G.W., Schlegel, H.B., Scuseria, G.E., Robb, M.A., Cheeseman, J.R., *et al.* (2016) Gaussian 16, Revision B.01. Gaussian, Inc., Wallingford.

[22] Kumar, A., Toal, S.E., DiGuiseppi, D., Schweitzer-Stenner, R. and Wong, B.M. (2020) Water-Mediated Electronic Structure of Oligopeptides Probed by Their UV Circular Dichroism, Absorption Spectra, and Time-Dependent DFT Calculations. *The Journal of Physical Chemistry B*, **124**, 2579-2590. https://doi.org/10.1021/acs.jpcb.0c00657

[23] O'boyle, N.M., Tenderholt, A.L. and Langner, K.M. (2008) Cclib: A Library for Package Independent Computational Chemistry Algorithms. *Journal of Computational Chemistry*, **29**, 839-845. https://doi.org/10.1002/jcc.20823

[24] Alauddin, M. and Ripa, J.D. (2022) Effect of Microhydration on the Peptide Backbone of N-Acetyl-Phenylalaninylamide (NAPA) Using IR, Raman and Vibrational Chiroptical Spectrosocpies (VCD, ROA): A Computational Study. *European Journal of Applied Sciences*, **10**, 617-638. https://doi.org/10.14738/aivp.104.12859

[25] Hubbard, R.E. and Haider, M.K. (2010) Hydrogen Bonds in Proteins: Role and Strength. Encyclopedia of Life Sciences. John Wiley & Sons, Ltd., Hoboken. https://www.els.net https://doi.org/10.1002/9780470015902.a0003011.pub2

[26] Micsonai, A., Bulyáki, É. and Kardos, J. (2021) BeStSel: From Secondary Structure Analysis to Protein Fold Prediction by Circular Dichroism Spectroscopy. In: Chen, Y.W. and Yiu, C.-P.B., Eds., *Structural Genomics*: *General Applications*, Vol. 2199, Springer, Berlin, 175-189. https://doi.org/10.1007/978-1-0716-0892-0_11

[27] Lan, S.C. and Liu, Y.H. (2015) TDDFT Study on the Excited-State Proton Transfer of 8-Hydroxyquinoline: Key Role of the Excited-State Hydrogen-Bond Strengthening. *Spectrochimica Acta Part A*: *Molecular and Biomolecular Spectroscopy*, **139**, 49-53. https://doi.org/10.1016/j.saa.2014.12.015

[28] Zhao, G.J. and Han, K.L. (2007) Ultrafast Hydrogen Bond Strengthening of the Photoexcited Fluorenone in Alcohols for Facilitating the Fluorescence Quenching. *The Journal of Physical Chemistry A*, **111**, 9218-9223. https://doi.org/10.1021/jp0719659